Goumans/Senden/van der Sloot, Editors
Waste Materials in Construction: Putting Theory into Practice

ELECTROKINETIC TRANSPORT IN NATURAL SOIL CORES

Douglas I. Stewart, L. Jared West, S. Richard Johnston and Andrew M. Binley

Abstract

Electrokinetic transport in natural soils has been investigated by applying a constant voltage across 500mm long by approximately 200mm diameter natural soil cores for periods of up to 8 weeks. Contaminant ions were circulated through a fluid filled reservoir between the anode and the soil, and distilled water was circulated through a similar reservoir adjacent to the cathode. During the experiments electrical current, voltage along the core, water flow rate, and anolyte and catholyte pH were monitored at regular intervals. Periodically, the electrical supply to the power electrodes was switched off and detailed electrical measurements were made using 68 monitoring electrodes positioned around the soil core, in order to produce three dimensional electrical resistivity images of the cores. After testing the cores were dissected and analysed for contaminant content, pore fluid composition, and pH.

Data are reported that show that zinc tracer transport is initially strongly retarded, with the zinc predominately sorbed to the soil. Initially zinc enters the anode region mainly by electromigration. This cannot change the pore fluid ionic strength due to charge balance constraints, and hence zinc influx is limited by initial ionic strength. However, after 8 weeks of testing, the ionic strength of the pore fluid in the anode half of the cores were significantly elevated by co-diffusion and electroosmotic advection of the anolyte into the core.

Introduction

Electrokinetic treatment is a developing technology for treating contaminated land. An electric current is passed through the soil causing migration of charged species towards collection wells. In fine grained soils pore water flow is also induced. Many laboratory studies have been performed to characterise electrokinetic transport, and the dominant processes have been identified (e.g. Eykholt and Daniel, 1994; Hamed et al., 1991; Yeung and Mitchell, 1993), and insitu field decontamination has been attempted (e.g. Lageman, 1993).

This paper reports a study investigating electrokinetic transport in natural soil cores. The aims were to characterise the interactions between natural soil and the contaminant, to investigate the influence of organic matter on electrokinetic transport, and to establish the usefulness of electrical resistivity tomography (ERT) for monitoring electrokinetic transport in the soil cores. ERT is a non-invasive technique where the spatial variation of resistivity is determined from measurements taken with an array of electrodes, which during insitu decontamination would be located in boreholes or along the ground surface.

Methodology

Core preparation

The cores used in this study were taken from the Lancaster University Hazelrigg field station. The sub-soil at this site is an orange/brown clayey loam containing rounded gravel particles up to 15cm in diameter. The mineralogy of this soil determined by quantitative XRD using a position sensitive detector (M. Batchelder, *pers. comm.*) is 46% quartz, 18% kaolinite, 14% montmorillonite, 11% illite, 5% feldspar, and 6% aluminium and iron hydroxides. The

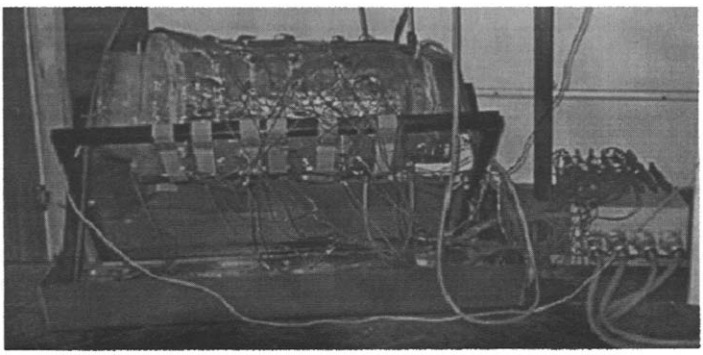

Figure 1: Soil core during electrokinetic testing

topsoil is brown/grey silty loam, 30-40cm deep, with most of the root material in the upper 10-20cm. The moisture content of these samples were all around 20% by weight.

Soil cores were carefully excavated by hand. The upper horizon of top-soil was removed (15-20cm, sufficient to remove visible plant mass). Each core was exposed by careful hand excavation, aiming for a sample diameter of 200mm (actual diameters were typically 240mm). Samples of the soil trimmings were taken for analysis every 10cm over the depth of the core. An electrode shell and geotextile were then placed on the top, and the entire core and electrode shell were coated with fibre-glass resin and fibre glass matting was applied. This was repeated twice more, and a final coat of resin was applied. The core was then left overnight for the resin coating to dry. The next day, it was under-cut and inverted, and sealed in polythene to prevent moisture loss.

Once in the laboratory, each core was trimmed, a second reservoir shell was positioned and sealed with glass fibre and resin. Next, 68 monitoring electrodes were inserted by drilling through the fibre-glass. Finally, the power electrodes and reservoir packing (a drainage geogrid) were inserted into the electrode shells, and the core was saturated by upward flow under approximately 1m head. Prior to testing, each core was positioned horizontally and the reservoirs were filled with the electrolyte solutions (see Figure 1).

Electrokinetic testing

During testing a constant voltage of 30V was applied between the power electrodes, and reservoir header-tank weights, electric current, and the voltage along the core were recorded at regular intervals. Test durations were nominally 2 weeks, 4 weeks, and 8 weeks. Periodically data were gathered for ERT image reconstruction (while electrical supply to the power electrodes was disconnected) using a computer controlled earth resistance meter. A total of 1860 'four-electrode' measurements were taken using combinations of the 68 monitoring electrodes, in each of four radial planes and two axial planes. Each 'four-electrode' measurement consists of driving current between two electrodes and measuring the resulting potential difference between the other two electrodes. Electrode polarisation is minimised by using a low frequency alternating current. ERT data acquisition took approximately 4 hours.

After testing, the cores were sliced into 50mm thick layers. Each slice was then photographed from the top and bottom, before the slice was homogenised. The pH of each slice was

measured by inserting a pH penetration electrode directly into the soil. Samples of each slice were then oven dried at 105°C to determine the moisture content, and the samples were analysed for elemental composition using X-ray Fluorescence Spectroscopy. Samples for XRF analysis were ground and compressed into pellets for analysis.

Pore water was extracted by centrifuge displacement (at approximately 50,000g) using an immiscible organic solvent (technical grade tetrachloroethylene). The pore water samples were passed through a 0.45 micron filter, and sub-samples to be analysed for metal content were acidified. The pore fluid pH and conductivity were measured. Pore fluid cation and silica concentrations were measured by Induction Coupled Plasma Atomic Emission Spectroscopy (ICP-AES), and anion concentrations were measured by Eluent Suppressed Ion Chromatography (using a carbonate eluent). Total carbonate concentrations in the pore fluids were measured separately using the flow injection analysis procedure described by Hall and Aller (1992).

Electrical resistivity tomography data processing.
A resistivity distribution was found for each set of four-electrode measurements by numerical non-linear inversion. The specimen was represented by a three-dimensional finite element mesh of 2288 triangular prismatic elements. This includes additional layers of elements at both ends of the specimen to account for the change in resistivity in the reservoir electrolyte. The resistivity of each finite element is treated as a variable for the inversion process. The data inversion employs a weighted least squares approach with regularisation. No constraining of the procedure using other measurements such as reservoir fluid conductivity was employed. More details of the three-dimensional ERT image reconstruction can be found in Binley et al. (1996).

Results
Data summarising each test is presented in Table 1. Voltage profiles taken from two rows of monitoring electrodes showed that the voltage applied across the cores were dropped steadily along their length. Variations in core conductivities were not discernible from this data. After problems with electrode degassing had been resolved, the electrical current through the cores was between 50 and 65mA and did not vary much during testing.

The moisture content in the anode half of the cores did not change much from field value of 20%, but in the upper, organic rich horizon it increased to between 30-40%. This increase in the moisture content was probably the result of pre-test core saturation. Electroosmotic flow data for test HR1 were erratic during optimisation of the test conditions. After optimisation, flow rates in specimens HR2 and HR3 varied between 100 and 300ml/day and tended to reduce during the test.

Table 1: Test details

Test	Duration (days)	Charge passed (kC)	Energy (kJ)	Average EO permeability ($cm^2/V.s$)
HR1	16	32	968	-
HR2	29	124	3,820	$1.6x10^{-5}$
HR3	57	277	8,464	$0.8x10^{-5}$

Note: Applied voltage was 30V in all three tests

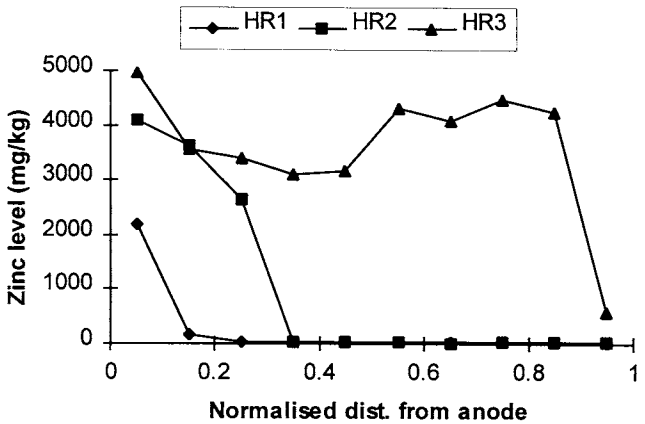

Figure 2: Total zinc level after core testing

Figure 2 shows total zinc profiles from tests HR1-3 (the background zinc level was below 40mg/kg everywhere). The anolyte was originally $Zn(NO_3)_2$ at a concentration of 1,000mg/l of zinc. Figure 2 shows that zinc was transported into the cores from the anolyte. After 2 weeks of voltage application, the zinc level had risen to over 2000mg/kg in the anode slice, with a much smaller increase in the next 50mm slice. After 4 weeks, the level in the anode slice had reached about 4000mg/kg, and zinc levels were also elevated in the next two slices. After 8 weeks, zinc levels were elevated to around 4000mg/kg in all but the cathode slice (where it had only increased to about 500mg/kg).

The initial soil pH decreased with depth from about 6.5 to 5. The soil pH after testing was typically about 5, with some increase towards the cathode, reaching pH 8 in the cathode slice of the core tested for longest (HR3). The pH of the catholyte was about 11 at the end of all the tests. Any Zn^{2+} approaching the cathode reservoir is therefore likely to have been precipitated.

Figure 3 shows the conductivity of the pore fluid from the background samples, and that from cores HR1-3 after testing (the values for normalised distances of 0 and 1 represent the reservoirs). In the background soil, the conductivity was highest (1600μS/cm) near the ground surface (corresponding to the cathode end of the cores), dropping over 250mm to a value of 200μS/cm. Pore fluid conductivity was steady at about 200μS/cm over the next 250mm (corresponding to the anode half of the cores). After 2 weeks of testing, there was little change in pore fluid conductivity. After 4 weeks, the pore fluid conductivity in the anode slice had increased to 700μS/cm, but with little change over the rest of the core. After 8 weeks of testing, the pore fluid conductivity in the anode half of the specimen had risen to nearly 1500μS/cm, with an even larger increase in the anode slice (3000μS/cm). The conductivity near the cathode was below the background value although this may reflect natural variability.

Figure 4 shows the pore fluid composition of the background samples, and at the end of tests HR1-3. In the background soil, the pore fluid has elevated concentrations of calcium and nitrate near the ground surface (corresponding to the cathode end of the cores). Other ions present in the pore fluid from background samples were sodium, potassium, chloride, sulphate

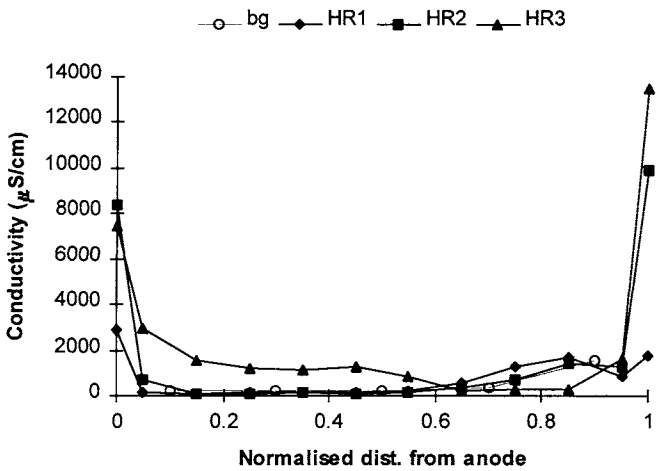

Figure 3: Conductivity of the extracted pore fluid

and carbonate. The elevated concentrations of Ca^{2+} and NO_3^- near the surface may reflect fertiliser application.

The data from core HR1 show that, after 2 weeks of testing, the pore fluid compositions are similar to those from the background soil. There were small increases in Zn^{2+} in the anode slice and of natural cations (K^+ and Na^+) in the cathode reservoir (relatively high calcium and nitrate concentrations in core HR1 probably reflect natural variability). The carbonate present in the cathode reservoir was probably HCO_3^- produced by interaction of electrolytically produced OH^- with atmospheric CO_2.

The data from core HR2 shows that, after 4 weeks of testing, the pore fluid compositions remained similar over most of the core, although there was an increase in Zn^{2+} in the 100mm nearest to the anode, and there was a significant increase in Ca^{2+} in the cathode reservoir. The data from core HR3 show that, after 8 weeks of testing, there were elevated Zn^{2+} levels in the two-thirds of the core closest to the anode and relatively low calcium and nitrate levels near the cathode. However, the pore fluid zinc levels remained much less than the total levels, which shows that most of the zinc was sorbed on contact with the soil.

Figure 5 is a plot of the Zn^{2+} in pore fluid against sorbed zinc, for those parts of all three cores which were composed of orange brown clay loam (i.e. excluding the topsoil). Despite the scatter, it can be seen that Zn(II) exhibits Freundlich sorption behaviour where the sorbed concentration is less than 4,000 mg/kg. Sorbed concentration did not exceed this value for higher pore fluid Zn^{2+} levels.

Figure 6 shows ERT images of core HR2 at intervals during testing (the elements representing the fluid reservoirs are included on the images). The main feature that is evident from the images is an increase in the catholyte conductivity due to electrolytic decomposition of water. The zone of conductivity increase in the images does not correspond exactly with the reservoir. This smearing is typical of ERT reconstruction for zones outside the electrode

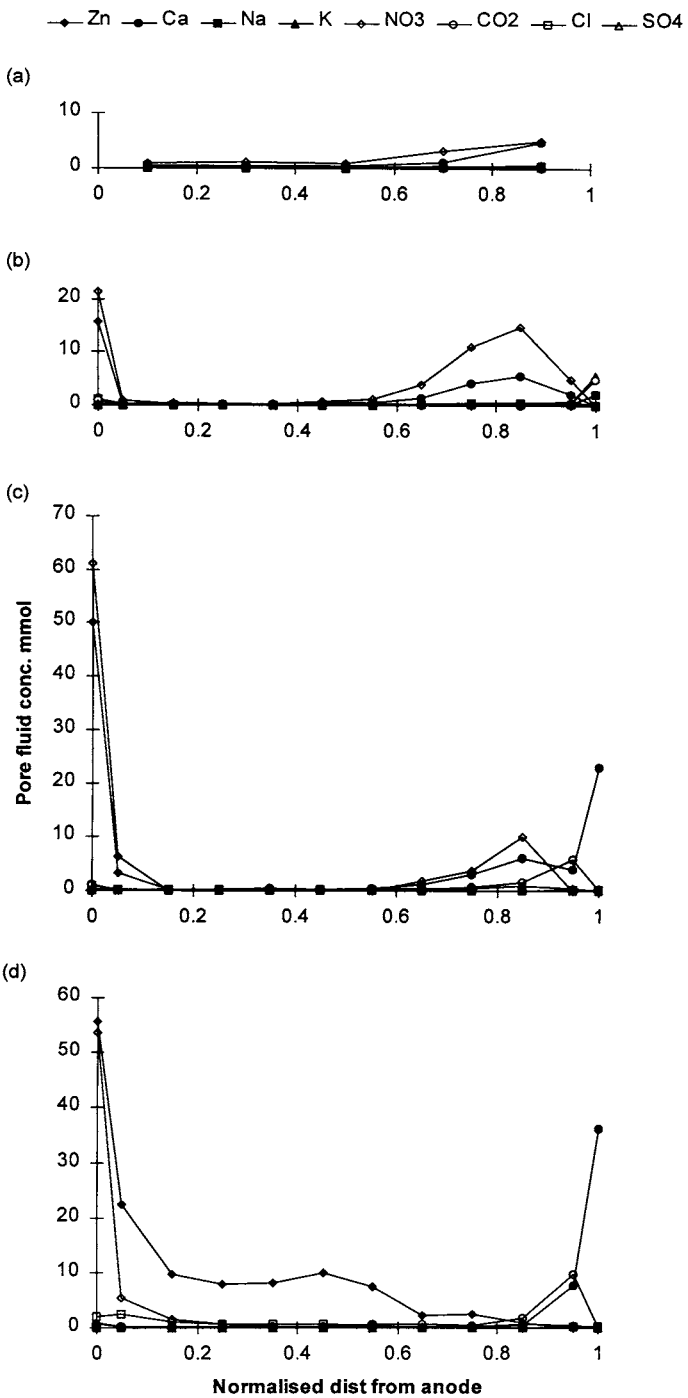

Figure 4: Composition of pore fluid (a) background, (b) HR1, (c) HR2, and (d) HR3

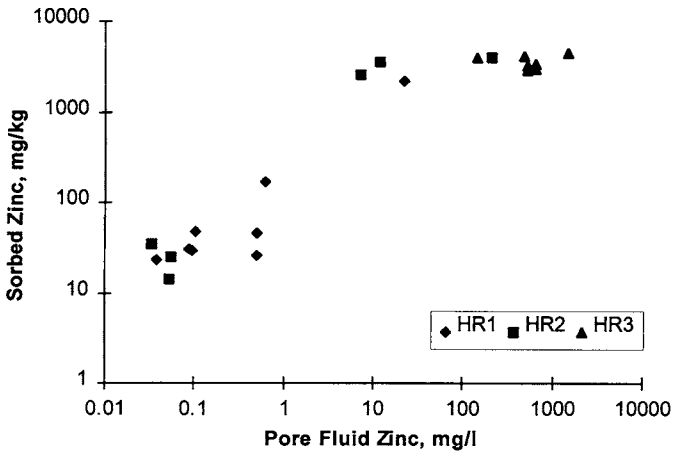

Figure 5: Pore fluid zinc concentration versus sorbed zinc for the clayey loam

arrays. Apart from this effect, the images show that the conductivity of the soil changed little over four weeks of testing.

Discussion

The measured pore fluid anions and cations in cores HR1 and HR2 are approximately in charge balance, indicating that all major ionic species have been identified. The measured ionic concentrations indicate a large excess of positively charged species in most of core HR3, and in the cathode reservoirs at the end of tests HR2 and HR3. The ion chromatograph results for these regions have unidentified peaks, the most significant of which had a relatively long residence time in the ion chromatography column. It is inferred that interaction of dissolved species with either the equipment or the soil released (as yet) unidentified anionic species, which migrate towards the anode.

Ideal solution conductivities were calculated from the ionic compositions using the dilute solution ionic mobilities (e.g. see Reiger, 1994). The ideal solution conductivities were typically higher than the measured pore fluid values, with the difference being largest where the ionic strength of the pore fluid was highest. This is consistent with the non-ideal behaviour of real electrolytes. The fractional contribution of each ion to the extracted pore fluid conductivity (its transport number) was calculated by assuming that (i) deviation from ideal behaviour within the pore fluid from each slice was the same for all ions and (ii) that all the major ionic species had been identified (this was not the case in core HR3). Within the cores, other effects such as diffusion and electroosmotic flow will modify transport numbers from those calculated for the extracted pore fluid (Alshawabkeh and Acar, 1996).

Figure 7 shows the major contributors to pore fluid conductivity (defined here as ions with transport numbers greater than 0.1) in the cores. Each sub-region indicated in Figure 7 has the same major contributors, although ionic concentrations varied substantially within sub-regions. These diagrams, although an approximation to the main charge carriers in the cores, are a useful for identifying the major processes during electrokinesis.

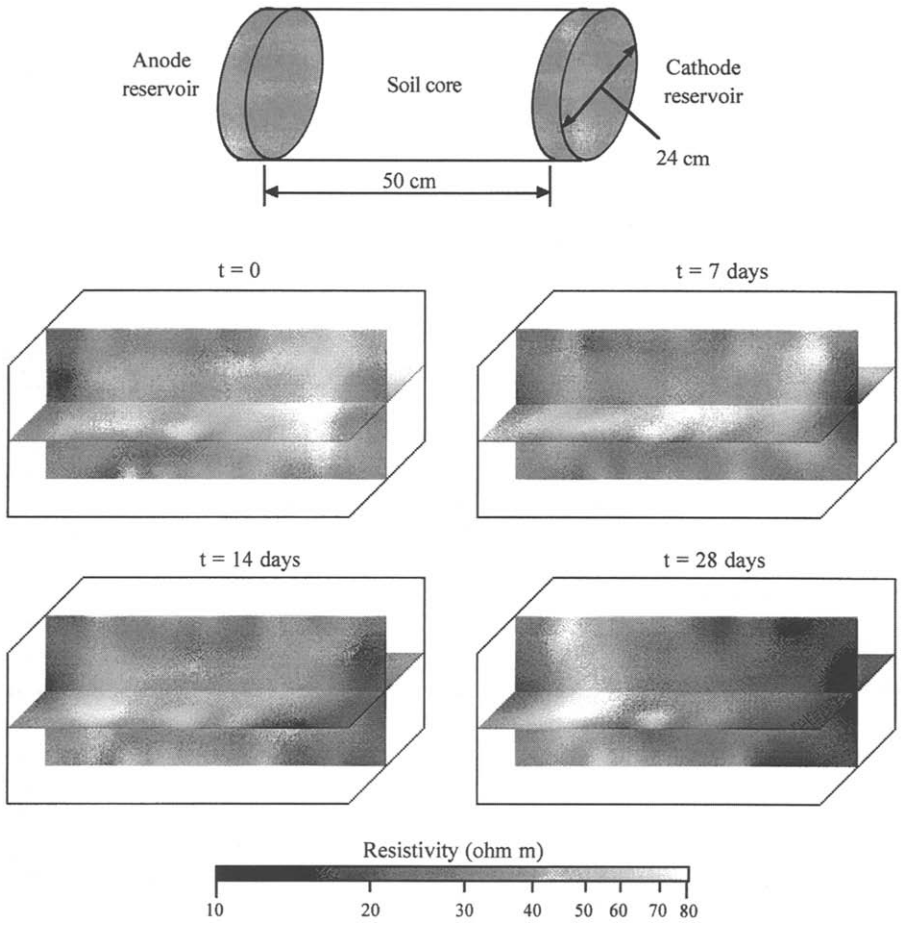

Figure 6: ERT images of core HR2

The pore fluid ionic strength after two weeks of electrokinesis had not changed much from background values, despite the increased ionic strength in the reservoir (anions produced by electrolysis and cations from the core raised the level in the cathode reservoir). The major processes that have occurred are electromigration of zinc from the anode reservoir, replacing the natural pore fluid calcium near the anode, and electromigration of HCO_3^- from the cathode reservoir, replacing nitrate and sulphate near the cathode.

After 4 weeks, the pattern remains similar, although increases in pore fluid strength are now apparent in both the anode and cathode slices. These local increases probably result from co-diffusion of anions and cations from the reservoirs, and in the anode slice, electroosmotic advection. Charge balance constraints prevent electromigration alone from causing these ionic strength variations (i.e. zinc can only enter the anode region by the electromigration mechanism at the same rate that natural cations are leaving it).

Background

Ca^{2+}	Ca^{2+}
NO_3^- SO_4^{2-}	NO_3^-

Anode Res.	Soil	Cath. Res.

Core HR1

Zn^{2+}	Zn^{2+} Ca^{2+}	Ca^{2+}	Ca^{2+}	Ca^{2+}	Ca^{2+}	Ca^{2+}	K^+ Na^+
NO_3^-	NO_3^- SO_4^{2-}	SO_4^{2-}	SO_4^{2-} NO_3^-	NO_3^- SO_4^{2-}	NO_3^-	NO_3^-	HCO_3^-

Core HR2

Zn^{2+}	Zn^{2+}	Zn^{2+}	Zn^{2+} Na^+	Ca^{2+}	Ca^{2+}	Ca^{2+}	Ca^{2+}	Ca^{2+}
NO_3^-	NO_3^-	SO_4^{2-} Cl^-	SO_4^{2-}	SO_4^{2-}	NO_3^- SO_4^{2-}	NO_3^-	HCO_3^-	?- HCO_3^-

Core HR3

Zn^{2+}	Zn^{2+}	Zn^{2+}	Zn^{2+}	Ca^{2+}	Ca^{2+}
NO_3^-	NO_3^- ?-	?-	SO_4^{2-} HCO_3^-	HCO_3^-	?-

?- indicates a region where there are unidentified anions.

Figure 7: Distribution of major contributors to extracted pore fluid conductivity

After 8 weeks, the ionic strength in the anode half of the core had risen substantially, but had reduced slightly in the cathode half. The ionic strength in the anode half rose as anions accumulating in this region (due to diffusion and electroosmotic advection) are not used up in precipitation or electrode reactions. This allowed higher concentrations of Zn^{2+} to enter from the reservoir

The pore fluid data show that the requirement for continuity of current and charge balance within the cores prevents electromigration alone from altering ionic strength (it can only substitute ions for others of equivalent charge). Changes in ionic strength at a specific location are therefore the result of advection or diffusion of electrolytes to that location, or dissociation/neutralisation and dissolution/precipitation reactions at that location.

Conclusions

① Initially, most of the zinc tracer entering the core was sorbed to the soil, whereas after 8 weeks of testing the sorption capacity had been exceeded across 60% of the specimen, permitting larger pore fluid zinc concentrations.

② Initially, there was little change in pore fluid conductivity. This is because the dominant transport process is electromigration, which alone cannot alter ionic strength.

③ Later, co-diffusion and electroosmotic advection of the anolyte into the cores progressively increased the ionic strength of the pore fluid.

Acknowledgements

The authors would like to acknowledge the support of the U.K. Engineering and Physical Sciences Research Council through grant GR/K57770. M Batchelder, Natural History Museum is thanked for the quantitative XRD analysis.

Appendix. References

Alshawabkeh, A.N. and Acar, Y.B. (1996). Electrokinetic remediation. II: theoretical model. ASCE Journal of Geotechnical Engineering, 122(3), 186-196.

Binley, A, Pinheiro, P. and Dickin F., (1996), Finite Element based Three-Dimensional Forward and Inverse Solvers for Electrical Impedance Tomography, In: Proc. Colloquium on Advances in Electrical Tomography, Computing and Control Division, IEE, Digest No. 96/143, p6/1-6/3, Manchester, June, 1996.

Eykholt, G.R. and Daniel D. E. (1994). Impact of system chemistry on electroosmosis of contaminated soils. ASCE Journal of Geotechnical Engineering, 120(5), 797-815.

Hall, P.O.J. and Aller, R.C. (1992). Rapid small volume flow injection analysis for total CO_2 and ammonium in marine and freshwaters. Limnology and Oceanography, **37**, 1113-1119.

Hamed, J., Acar, Y.B. and Gale, J.G. (1991). Pb(II) removal from kaolinite by electro-kinetics. ASCE. Journal of Geotechnical Engineering, 117(2), 241-271.

Lageman, R. (1993). Electroreclamation: applications in the Netherlands. Environmental Science and Technology, 27, 2648-2650.

Reiger, P.H. (1994). Electrochemistry. Chapman and Hall, 2nd ed.

Yeung, A.T. and Mitchell, J.K. (1993). Coupled fluid, electrical and chemical flows in soil. Geotechnique 43(1), 121-134.